1 Torque Data

The following is the list of data runs used in the final torque fit to pure Newtonian and Netwonian + Yukawa models. We have rotated the torque values into a single in-phase component and subtracted systematic torques.

s [μm]	N_{120} [fNm]	N_{18} [fNm]	N_{54} [fNm]
168.8 ± 0.9	0.8180 ± 0.0108	0.9557 ± 0.0080	0.1085 ± 0.0056
79.3 ± 0.8	1.4375 ± 0.0191	1.0904 ± 0.0111	0.1186 ± 0.0086
64.4 ± 0.8	1.5724 ± 0.0650	1.0557 ± 0.0201	0.1281 ± 0.0177
64.6 ± 0.8	1.5752 ± 0.0478	1.0569 ± 0.0370	0.1188 ± 0.0256
53.7 ± 0.8	1.7729 ± 0.3802	1.0388 ± 0.0753	0.1245 ± 0.0490
63.0 ± 0.8	1.5606 ± 0.0408	1.0754 ± 0.0332	0.1175 ± 0.0204
56.2 ± 0.9	1.7324 ± 0.0399	1.1148 ± 0.0731	0.1393 ± 0.0385
370.6 ± 1.0	0.2346 ± 0.0100	0.7881 ± 0.0099	0.0510 ± 0.0077
370.6 ± 1.0	0.2189 ± 0.0131	0.7766 ± 0.0093	0.0687 ± 0.0075
987.8 ± 1.3	0.0069 ± 0.0213	0.4388 ± 0.0120	0.0094 ± 0.0076
64.7 ± 0.9	1.5373 ± 0.0577	1.0706 ± 0.0260	0.1045 ± 0.0215
58.6 ± 0.9	1.6600 ± 0.0267	1.1424 ± 0.0187	0.1339 ± 0.0125
219.8 ± 0.9	0.5859 ± 0.0151	0.9347 ± 0.0086	0.0809 ± 0.0104
421.2 ± 1.0	0.1626 ± 0.0169	0.7639 ± 0.0104	0.0510 ± 0.0081
575.7 ± 1.1	0.0731 ± 0.0181	0.6643 ± 0.0088	0.0502 ± 0.0054
59.8 ± 0.9	1.6686 ± 0.0322	1.0626 ± 0.0200	0.1466 ± 0.0147
72.5 ± 0.8	1.5122 ± 0.0236	1.0902 ± 0.0247	0.1117 ± 0.0178
69.0 ± 0.9	1.5455 ± 0.0195	1.0858 ± 0.0242	0.1282 ± 0.0165
135.8 ± 0.9	1.0205 ± 0.0241	0.9919 ± 0.0149	0.1141 ± 0.0119
1236.0 ± 1.3	0.0225 ± 0.0147	0.3746 ± 0.0114	0.0073 ± 0.0079
59.2 ± 0.9	1.6777 ± 0.0514	1.0844 ± 0.0428	0.1332 ± 0.0230
54.8 ± 0.9	1.7204 ± 0.1427	1.0989 ± 0.1329	0.1528 ± 0.0459
58.4 ± 0.8	1.8813 ± 0.3439	0.9730 ± 0.1403	0.0666 ± 0.1787
72.2 ± 0.9	1.4672 ± 0.0684	1.1208 ± 0.0527	0.0791 ± 0.0265
70.1 ± 0.8	1.4862 ± 0.0652	1.1209 ± 0.0494	0.1124 ± 0.0214
85.5 ± 0.8	1.3993 ± 0.0162	1.0550 ± 0.0130	0.1209 ± 0.0069
67.5 ± 0.8	1.5264 ± 0.1305	0.6600 ± 0.3378	0.1923 ± 0.1494
67.5 ± 0.9	1.6371 ± 0.0849	0.9937 ± 0.0820	0.2046 ± 0.0322
84.4 ± 0.8	1.3685 ± 0.0252	1.0500 ± 0.0285	0.1330 ± 0.0085
62.2 ± 0.8	1.0593 ± 0.7301	1.1488 ± 0.2657	0.8180 ± 1.4401
2113.3 ± 1.3	-0.0011 ± 0.0182	0.1591 ± 0.0146	-0.0055 ± 0.0136
61.5 ± 0.8	1.7197 ± 0.3962	1.1179 ± 0.1198	-0.0462 ± 0.7454
2552.2 ± 1.3	-0.0351 ± 0.0231	0.1142 ± 0.0065	0.0145 ± 0.0294
122.8 ± 0.8	1.0930 ± 0.0114	0.9985 ± 0.0072	0.1029 ± 0.0046
322.6 ± 0.9	0.3015 ± 0.0164	0.8180 ± 0.0089	0.0741 ± 0.0067
487.8 ± 1.0	0.1208 ± 0.0098	0.7185 ± 0.0083	0.0575 ± 0.0056
61.1 ± 0.8	1.7604 ± 0.1269	1.0616 ± 0.0433	-0.1992 ± 0.2587
61.0 ± 0.8	1.5952 ± 0.1378	1.1022 ± 0.0447	-0.0178 ± 0.2692
60.9 ± 0.8	1.4965 ± 0.1189	1.0857 ± 0.0429	0.2587 ± 0.2365

s [μm]	N_{120} [fNm]	N_{18} [fNm]	N_{54} [fNm]
1525.6 ± 1.3	-0.0030 ± 0.0252	0.2744 ± 0.0066	0.0298 ± 0.0263
126.1 ± 0.8	1.0632 ± 0.0149	1.0118 ± 0.0081	0.1033 ± 0.0077
108.1 ± 0.8	1.2030 ± 0.0184	1.0353 ± 0.0085	0.1291 ± 0.0051
70.2 ± 0.8	1.5286 ± 0.0724	1.0609 ± 0.0299	0.0851 ± 0.1453
70.1 ± 0.8	1.4778 ± 0.0698	1.1080 ± 0.0289	0.1856 ± 0.1402
99.2 ± 0.8	1.2642 ± 0.0117	1.0071 ± 0.0094	0.1121 ± 0.0069
91.9 ± 0.8	1.3506 ± 0.0231	1.0180 ± 0.0173	0.1190 ± 0.0080
781.3 ± 1.2	0.0255 ± 0.0137	0.5432 ± 0.0052	0.0196 ± 0.0051
61.4 ± 0.9	1.5774 ± 0.5738	1.3194 ± 0.2185	0.2137 ± 1.1771
60.9 ± 0.8	1.6578 ± 0.4479	1.0248 ± 0.1558	0.2089 ± 0.8927
61.0 ± 0.8	0.4716 ± 0.7331	0.9970 ± 0.3106	2.5946 ± 1.4803
61.0 ± 0.8	1.9439 ± 0.8181	1.2225 ± 0.3755	-0.4906 ± 1.6343
692.5 ± 1.1	0.0324 ± 0.0114	0.5912 ± 0.0064	0.0252 ± 0.0054
261.3 ± 0.9	0.4571 ± 0.0095	0.8846 ± 0.0066	0.0774 ± 0.0050
299.5 ± 0.9	0.3637 ± 0.0238	0.8465 ± 0.0085	0.0753 ± 0.0069
106.6 ± 0.8	1.2157 ± 0.0141	1.0131 ± 0.0078	0.1063 ± 0.0052
3040.4 ± 1.3	0.0290 ± 0.0363	0.0794 ± 0.0091	0.0303 ± 0.0439
91.5 ± 0.8	1.3472 ± 0.0206	1.0599 ± 0.0083	0.1209 ± 0.0056
79.4 ± 1.0	1.4479 ± 0.0176	1.0636 ± 0.0100	0.1296 ± 0.0065
71.7 ± 0.8	1.5303 ± 0.0348	1.0430 ± 0.0393	0.1319 ± 0.0153
61.7 ± 0.8	2.2984 ± 0.3353	0.8129 ± 0.1171	-1.2318 ± 0.6897
61.2 ± 0.8	1.2821 ± 0.2338	1.0789 ± 0.1003	0.7464 ± 0.4899
55.1 ± 0.8	1.5864 ± 0.4102	1.0244 ± 0.1279	0.2270 ± 0.8200
879.5 ± 1.2	0.0376 ± 0.0251	0.4912 ± 0.0064	0.0294 ± 0.0318
73.4 ± 0.8	1.4824 ± 0.1438	1.0121 ± 0.0536	-0.1341 ± 0.2881
73.3 ± 0.8	1.4429 ± 0.0743	1.0188 ± 0.0260	0.0593 ± 0.1538
73.2 ± 0.8	1.4820 ± 0.0837	1.0025 ± 0.0300	0.0307 ± 0.1697
72.5 ± 0.8	1.4496 ± 0.0459	1.0293 ± 0.0160	0.0528 ± 0.0912
72.5 ± 0.9	1.4777 ± 0.0493	1.0448 ± 0.0162	0.0346 ± 0.0987
72.3 ± 0.8	1.4177 ± 0.0303	1.0569 ± 0.0114	0.1150 ± 0.0550
72.5 ± 0.8	1.4693 ± 0.0328	1.0684 ± 0.0108	0.0422 ± 0.0623
59.8 ± 0.8	1.6276 ± 0.0500	1.0655 ± 0.0163	0.0608 ± 0.0981
131.8 ± 0.8	1.0102 ± 0.0080	0.9975 ± 0.0092	0.1077 ± 0.0034
61.7 ± 0.8	1.6886 ± 0.0549	1.0581 ± 0.0191	-0.0375 ± 0.1064
61.4 ± 0.8	1.6051 ± 0.0236	1.0684 ± 0.0083	0.1588 ± 0.0427
56.5 ± 0.8	1.7163 ± 0.2340	1.0059 ± 0.0799	0.0207 ± 0.4759
164.7 ± 0.8	0.8214 ± 0.0098	0.9615 ± 0.0106	0.0955 ± 0.0064
51.6 ± 0.8	1.5804 ± 0.1690	0.8501 ± 0.1885	0.2172 ± 0.0749
64.5 ± 0.8	1.5917 ± 0.0150	1.0774 ± 0.0137	0.1263 ± 0.0063
60.1 ± 0.8	1.6429 ± 0.0227	1.0824 ± 0.0140	0.1304 ± 0.0099
59.3 ± 0.8	1.6280 ± 0.0223	1.1014 ± 0.0203	0.1286 ± 0.0148
55.8 ± 0.8	1.5618 ± 0.2460	1.0413 ± 0.2891	0.1698 ± 0.1221
50.4 ± 0.8	0.3144 ± 1.9727	-0.5569 ± 1.4281	0.1692 ± 0.6707
50.3 ± 0.8	0.6953 ± 1.5283	2.6129 ± 1.1657	-0.4992 ± 0.5137
55.4 ± 0.8	1.6597 ± 0.1473	1.0774 ± 0.1928	0.1562 ± 0.0803

s [μm]	N_{120} [fNm]	N_{18} [fNm]	N_{54} [fNm]
55.3 ± 0.9	1.7781 ± 0.1529	1.2075 ± 0.1029	0.1691 ± 0.0343
59.5 ± 0.8	1.6527 ± 0.0588	1.1367 ± 0.0324	0.1248 ± 0.0159
59.1 ± 0.8	1.5932 ± 0.0585	0.9687 ± 0.0506	0.1279 ± 0.0149
58.1 ± 0.8	1.6531 ± 0.0268	1.0684 ± 0.0262	0.1549 ± 0.0127
198.5 ± 0.9	0.6485 ± 0.0156	0.9337 ± 0.0080	0.0825 ± 0.0071
73.1 ± 0.8	1.5021 ± 0.0281	1.0740 ± 0.0147	0.1136 ± 0.0064
73.0 ± 0.8	1.4880 ± 0.0326	1.0990 ± 0.0253	0.1429 ± 0.0119
74.3 ± 0.8	1.4787 ± 0.0254	1.0791 ± 0.0249	0.1245 ± 0.0091
74.1 ± 0.8	1.5035 ± 0.0423	1.0982 ± 0.0221	0.1347 ± 0.0112
200.3 ± 0.9	0.6653 ± 0.0120	0.9442 ± 0.0059	0.0868 ± 0.0042
73.9 ± 0.8	1.4834 ± 0.0170	1.0582 ± 0.0158	0.1446 ± 0.0113

2 Gravitational Model and Fit Parameters

The Newtonian torque model was based on the cylindrically symmetric Fourier-Bessel calculations with corrections for angular and radial misalignments, geometry and metrology errors, and a calibration uncertainty.

We calculated the Fourier-Bessel torques over a set of separations covering the experimental range with the platinum density fixed at its nominal value $\rho_{nom} = 21.45 g/cm^3$ and the glue density at our measured value of $1.162 g/cm^3$. The thickness, angular, and radial geometry of the wedges were obtained from Smartscope measurements. We defined the overcut parameter, ϵ, to account for roughness of the platinum surfaces cut by the EDM, so that a positive overcut increased the area of the wedges equally in all directions, see figure 2. We used a third-order spline interpolation to asses the torque at a given separation and combination of fit parameters $(t_a, t_p, \rho_g, \epsilon)$. We then corrected for the change in the density computed with the measured missing masses (m_p, m_a) by scaling relative to the nominal density.

We corrected for the effect of radial misalignments of both the attractor and pendulum test-mass from the turntable rotation axis (r_a and r_j, respectively) using an empirical function derived from Monte-Carlo calculations of torque radial dependence. The Monte-Carlo calculations were computed for each harmonic at various separations, radial offsets, and for various λ including Newtonian gravity. Measurements of the horizontal location of the 120ω torque maximum determined the position of the attractor rotation axis (x_0, y_0), and the pendulum position (x_j, y_j) was recorded for each data run. The radial misalignment of the attractor test-mass was found with the Smartscope. The two contributions did not add as one displacement since the direction of the attractor test-mass displacement changed with the turntable rotation.

We corrected for tilts of the attractor and pendulum test-masses relative to the rotation axis (Ψ_A and Ψ_P respectively) by including a second-order effect from the root-mean-square (RMS) separation. The tilt corrections summed in quadrature since the direction of attractor tilt changed with the turntable rotation.

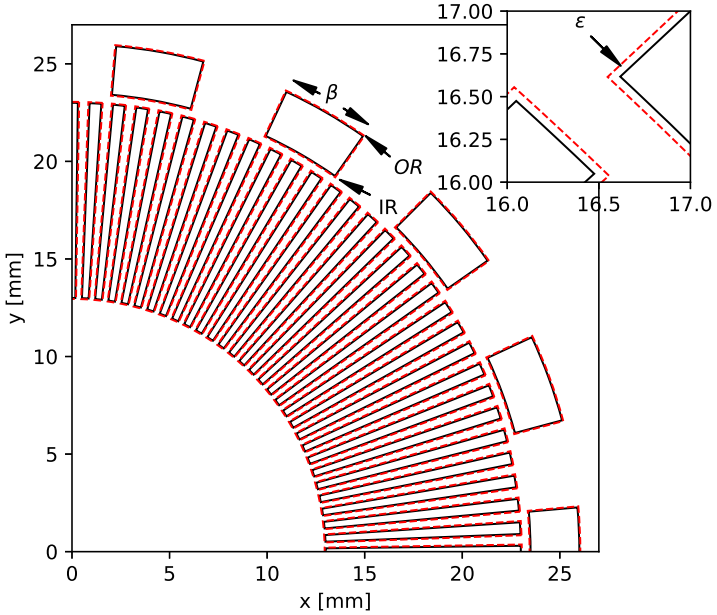

Figure 1: Geometric parameters of the wedge patterns. The subtended angle, β, and the inner and outer radii were computed at nominal values found by measurements with the Smartscope and adjusted with the overcut parameter, ϵ.

Finally, we scaled the predicted torques by a factor γ to account for the autocollimator calibration. This factor was determined by measurements with the external calibration turntable. The total Newtonian ($\lambda = \infty$) and Yukawa torque model were given by

$$\widetilde{N}_m(\vec{\zeta}_j, \vec{\eta}, \lambda) = \overbrace{\gamma}^{\text{Cal. scale}} \overbrace{\left(\frac{m_p}{t_p A_p \rho_{nom}}\right)\left(\frac{m_a}{t_a A_a \rho_{nom}}\right)}^{\text{fit density correction}} \overbrace{R_m(r_j, r_a, s_j, \lambda)}^{\text{Radial misalignment}} \times$$

$$\left[\underbrace{\overline{N}_m(s_j, t_p, t_a, \rho_g, \epsilon, \lambda)}_{\text{Fourier-Bessel Torque}} + \underbrace{\frac{1}{2}(\Delta s_m^2(\Psi_A) + \Delta s_m^2(\Psi_P))\frac{d^2\overline{N}_m(s_j, t_p, t_a, \rho_g, \epsilon, \lambda)}{ds_j^2}}_{\text{2nd Order RMS separation correction}}\right]$$

The complete set of model parameters were defined as:

- $m_{p,120}$, $m_{p,18}$, $m_{a,120}$, $m_{a,18}$: The missing mass from the pendulum and attractor 18- and 120-fold patterns.

- $t_{p,120}$, $t_{p,18}$, $t_{a,120}$, $t_{a,18}$: The thickness of the pendulum and attractor 18- and 120-fold wedges.

- x_0, y_0: The horizontal location of the attractor turntable rotation axis as measured with the dial indicators of the pendulum translation stages. This location was determined by maximizing the 120ω torque at a constant separation. The pendulum dial indicator positions were recorded for each data run $[x_j, y_j, z_j]$ so the radial misalignment of the pendulum is $r_j = \sqrt{(x_j - x_0)^2 + (y_j - y_0)^2}$.

- s_0: Contribution to the total separation from the screen and epoxy film thickness, so the total separation for a given run is, $s_j = z_{p,j} + z_a + s_0$. The dial indicator position z_j and pendulum-screen capacitance C_j for each run determine the pendulum separation to the screen $z_{p,j}(z_j, C_j)$. The attractor-screen position z_a was determined via screen actuator position and attractor-screen capacitance. The addition of the s_0 parameter accounts for the thickness of the epoxy uniformly coating each test-mass along with the screen thickness determined by touch probe measurements.

- ρ_g: Density of the Stycast 1266 epoxy with Loctite Catalyst 23LV hardener that fills the gaps in the platinum wedges. The mistaken use of the wrong hardener required a separate measurement of the epoxy density.

- Ψ_a: The tilt angle of the attractor test-mass with respect to the turntable rotation axis.

- Ψ_p: The tilt angle of the pendulum test-mass with respect to the turntable rotation axis.

- ϵ: The overcut parameter which accounts for roughness of the platinum surfaces cut by the EDM, so that a positive overcut increased the area of the wedges equally in all directions

- r_a: The radial misalignment (runout) of the attractor 120-fold pattern relative to the turntable axis of rotation.

- γ: The overall scale factor determined from the gravititational torque calibration accounting for autocollimator calibration uncertainty.

The phase of the pendulum pattern was defined relative to the attractor pattern when the attractor turntable was at the index mark. This phase was fixed at the value that maximized the 18ω and 120ω signals for the entire dataset and was determined to $\pm 0.0096°$.

Parameter	Measured	Fit	Units	χ^2
x_0	-0.130 ± 0.004	-0.129 ± 0.003	mm	0.10
y_0	-2.138 ± 0.003	-2.136 ± 0.003	mm	0.48
s_0	13.1 ± 1.4	14.1 ± 0.8	μm	0.48
$m_{A,120}$	1.19856 ± 0.00013	1.19856 ± 0.00013	mg	0.00
$m_{A,18}$	0.40955 ± 0.00010	0.40955 ± 0.00010	mg	0.00
$m_{P,120}$	0.65749 ± 0.00013	0.65749 ± 0.00013	mg	0.00
$m_{P,18}$	0.22402 ± 0.00008	0.22402 ± 0.00008	mg	0.00
$t_{A,120}$	98.58 ± 0.70	98.69 ± 0.67	μm	0.03
$t_{A,19}$	98.62 ± 0.64	98.61 ± 0.64	μm	0.00
$t_{P,120}$	54.33 ± 0.49	54.39 ± 0.48	μm	0.02
$t_{P,18}$	54.13 ± 0.56	54.12 ± 0.56	μm	0.00
ρ_g	1.162 ± 0.004	1.163 ± 0.004	g/cm^3	0.00
Ψ_A	58 ± 9	58 ± 9	μrad	0.00
Ψ_P	0 ± 45	0 ± 45	μrad	0.00
ϵ	0.2 ± 0.4	0.4 ± 0.4	μm	0.12
r_A	7.5 ± 1.8	7.5 ± 1.8	μm	0.00
γ	1.012 ± 0.005	1.010 ± 0.002	–	0.29

We began by fitting the purely Newtonian model ($\widetilde{N}_m(\vec{\zeta_j}, \vec{\eta}, \infty)$) with the complete set of model parameters allowed to float and found that only a small subset of five parameters contributed significantly to χ^2. We then performed a simpler fit with only x_0, y_0, s_0, ϵ and γ varying and the remaining parameters fixed by their measurements.

Parameter	Measured	Fit	Units	χ^2
x_0	-0.130 ± 0.004	-0.129 ± 0.003	mm	0.10
y_0	-2.138 ± 0.003	-2.136 ± 0.003	mm	0.48
s_0	13.1 ± 1.4	14.1 ± 0.7	μm	0.55
ϵ	0.2 ± 0.4	0.4 ± 0.4	μm	0.14
γ	1.012 ± 0.005	1.010 ± 0.002	–	0.28

3 χ^2 vs. λ

We first tested the pure Newtonian model ($\lambda = \infty$) and found $\chi^2 = 274.99$ with $\nu = 285$ degrees of freedom. We then searched for the inclusion of a single Yukawa torque with λ between 5μm and 9mm. None of the Yukawa potentials were preferred at 2σ ($\Delta\chi^2 = 6.17$) with the best fit $\Delta\chi^2 = 3.3$ at $\lambda = 7.1\mu$m. We placed positive and negative exclusion limits based on the $\Delta\chi^2 = 6.17$ surface. We placed a 2σ limit on the absolute value of α at each λ by finding the $|\alpha_{95}|$ at which

$$\int_{-|\alpha_{95}|}^{|\alpha_{95}|} \mathcal{N}(\alpha^*, \sigma_\alpha) d\alpha = 0.95$$

where $\mathcal{N}(\alpha^*, \sigma_\alpha)$ is a normal distribution with mean and standard deviation given by the best fit value with uncertainty, $\alpha^* \pm \sigma_\alpha$.

λ [mm]	α^*	$\pm$	σ_α	$+\alpha_{95}$	$-\alpha_{95}$	$\lvert\alpha_{95}\rvert$	χ^2
0.0050	4.09×10^6	$\pm$	2.58×10^6	1.18×10^7	-1.63×10^6	8.45×10^6	271.89
0.0056	8.6×10^5	$\pm$	5.29×10^5	2.4×10^6	-3.35×10^5	1.75×10^6	271.78
0.0063	1.93×10^5	$\pm$	1.17×10^5	5.31×10^5	-6.18×10^4	3.9×10^5	271.72
0.0071	4.76×10^4	$\pm$	2.86×10^4	1.29×10^5	-1.53×10^4	9.58×10^4	271.71
0.0079	1.5×10^4	$\pm$	8.96×10^3	3.99×10^4	-4.88×10^3	3.01×10^4	271.73
0.0089	4.52×10^3	$\pm$	2.71×10^3	1.19×10^4	-1.5×10^3	9.1×10^3	271.79
0.0100	1.53×10^3	$\pm$	923	3.99×10^3	-520	3.09×10^3	271.86
0.0110	668	$\pm$	406	1.73×10^3	-232	1.35×10^3	271.92
0.0130	176	$\pm$	108	465	-63.5	359	272.04
0.0140	102	$\pm$	63	268	-37.3	208	272.09
0.0160	40.3	$\pm$	25.3	106	-15.2	83	272.19
0.0180	18.9	$\pm$	12	49.4	-7.36	39.2	272.27
0.0200	10.1	$\pm$	6.47	26.3	-4.02	21	272.34
0.0220	5.91	$\pm$	3.83	15.4	-2.41	12.4	272.41
0.0250	3.03	$\pm$	2	7.9	-1.27	6.4	272.50
0.0280	1.75	$\pm$	1.17	4.51	-0.886	3.73	272.59
0.0320	0.963	$\pm$	0.661	2.56	-0.507	2.08	272.71
0.0350	0.663	$\pm$	0.464	1.77	-0.36	1.45	272.81
0.0400	0.394	$\pm$	0.286	1.06	-0.226	0.877	272.97
0.0450	0.257	$\pm$	0.194	0.699	-0.157	0.585	273.13
0.0500	0.179	$\pm$	0.142	0.494	-0.117	0.419	273.30
0.0560	0.124	$\pm$	0.104	0.35	-0.0884	0.3	273.49
0.0630	0.0862	$\pm$	0.078	0.251	-0.0685	0.218	273.71
0.0710	0.0601	$\pm$	0.06	0.183	-0.055	0.162	273.94
0.0790	0.0437	$\pm$	0.0485	0.14	-0.0469	0.126	274.14
0.0890	0.0304	$\pm$	0.0393	0.106	-0.0407	0.097	274.36
0.1000	0.021	$\pm$	0.0326	0.0813	-0.0365	0.0766	274.56
0.1100	0.0151	$\pm$	0.0285	0.0666	-0.034	0.0641	274.70
0.1300	0.0076	$\pm$	0.0231	0.048	-0.0312	0.0487	274.88
0.1400	0.00511	$\pm$	0.0213	0.042	-0.0304	0.0439	274.93
0.1600	0.00157	$\pm$	0.0187	0.0336	-0.0293	0.0376	274.98
0.1800	-0.000748	$\pm$	0.0169	0.0282	-0.0287	0.0339	274.99
0.2000	-0.00235	$\pm$	0.0157	0.0245	-0.0284	0.0317	274.97
0.2200	-0.00351	$\pm$	0.0147	0.0219	-0.0281	0.0303	274.94
0.2500	-0.00471	$\pm$	0.0137	0.0192	-0.0279	0.029	274.88
0.2800	-0.00552	$\pm$	0.013	0.0174	-0.0278	0.0282	274.81
0.3200	-0.00624	$\pm$	0.0123	0.0157	-0.0276	0.0275	274.74
0.3500	-0.00661	$\pm$	0.0119	0.0148	-0.0275	0.0271	274.69
0.4000	-0.00701	$\pm$	0.0114	0.0137	-0.0273	0.0265	274.62
0.4500	-0.00723	$\pm$	0.011	0.0129	-0.0269	0.026	274.57
0.5000	-0.00731	$\pm$	0.0107	0.0123	-0.0265	0.0254	274.53
0.5600	-0.00728	$\pm$	0.0103	0.0117	-0.0259	0.0247	274.49
0.6300	-0.00713	$\pm$	0.00982	0.0111	-0.025	0.0238	274.47
0.7100	-0.00685	$\pm$	0.00936	0.0105	-0.0239	0.0227	274.46

λ [mm]	$\alpha^* \pm \sigma_\alpha$	$+\alpha_{95}$	$-\alpha_{95}$	$\lvert\alpha_{95}\rvert$	χ^2
0.7900	-0.00653 ± 0.00893	0.01	-0.0228	0.0217	274.46
0.8900	-0.00612 ± 0.00845	0.00953	-0.0215	0.0205	274.47
1.0000	-0.00569 ± 0.00796	0.00903	-0.0201	0.0192	274.49
1.1000	-0.00534 ± 0.00763	0.00872	-0.0192	0.0183	274.50
1.3000	-0.00478 ± 0.00706	0.00816	-0.0175	0.0168	274.53
1.4000	-0.00456 ± 0.00683	0.00795	-0.0169	0.0162	274.55
1.6000	-0.00421 ± 0.00648	0.0076	-0.0158	0.0152	274.57
1.8000	-0.00395 ± 0.00621	0.00734	-0.015	0.0145	274.59
2.0000	-0.00375 ± 0.00599	0.00712	-0.0144	0.014	274.60
2.2000	-0.0036 ± 0.00585	0.00699	-0.014	0.0136	274.61
2.5000	-0.00344 ± 0.00567	0.00682	-0.0135	0.0131	274.63
2.8000	-0.00332 ± 0.00555	0.00669	-0.0132	0.0128	274.64
3.2000	-0.0032 ± 0.00543	0.00657	-0.0128	0.0125	274.64
3.5000	-0.00314 ± 0.00536	0.00651	-0.0126	0.0123	274.65
4.0000	-0.00307 ± 0.00526	0.0064	-0.0124	0.0121	274.65
4.5000	-0.00303 ± 0.00523	0.00637	-0.0123	0.012	274.66
5.0000	-0.00299 ± 0.00517	0.0063	-0.0121	0.0118	274.66
5.6000	-0.00295 ± 0.00515	0.0063	-0.012	0.0118	274.66
6.3000	-0.00293 ± 0.00512	0.00627	-0.012	0.0117	274.67
7.1000	-0.0029 ± 0.0051	0.00625	-0.0119	0.0116	274.67
7.9000	-0.00289 ± 0.00508	0.00623	-0.0119	0.0116	274.67
8.9000	-0.00288 ± 0.00507	0.00621	-0.0118	0.0116	274.67